

Molecular Structure–Intersystem Crossing Relationship of Heavy-Atom-Free BODIPY Triplet Photosensitizers

Shaomin Ji,^{*,†,‡} Jie Ge,^{†,‡} Daniel Escudero,[§] Zhijia Wang,[‡] Jianzhang Zhao,^{*,‡} and Denis Jacquemin^{*,§,||}

[†]Key Laboratory of Low Dimensional Materials & Application Technology, Ministry of Education, School of Materials Science and Engineering, Xiangtan University, Xiangtan 411105, P. R. China

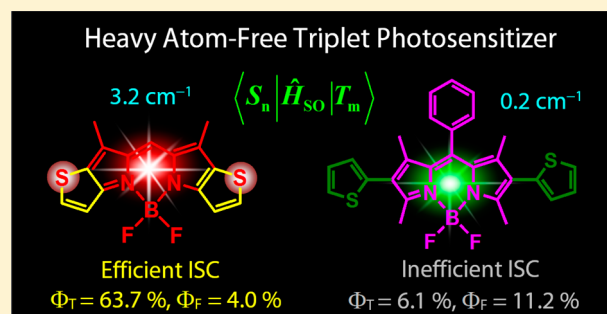
[‡]State Key Laboratory of Fine Chemicals, School of Chemical Engineering, Dalian University of Technology, E-208 West Campus, 2 Ling Gong Road, Dalian 116024, P. R. China

[§]CEISAM UMR CNRS 6230, Université de Nantes, 2 rue de la Houssinière, BP 92208, 44322 Nantes Cedex 3, France

^{||}Institut Universitaire de France, 103 boulevard St Michel, 75005 Paris Cedex 5, France

Supporting Information

ABSTRACT: A thiophene-fused BODIPY chromophore displays a large triplet-state quantum yield ($\Phi_T = 63.7\%$). In contrast, when the two thienyl moieties are not fused into the BODIPY core, intersystem crossing (ISC) becomes inefficient and Φ_T remains low ($\Phi_T = 6.1\%$). First-principles calculations including spin–orbit coupling (SOC) were performed to quantify the ISC. We found larger SOC and smaller singlet–triplet energy gaps for the thiophene-fused BODIPY derivative. Our results are useful for studies of the photochemistry of organic chromophores.



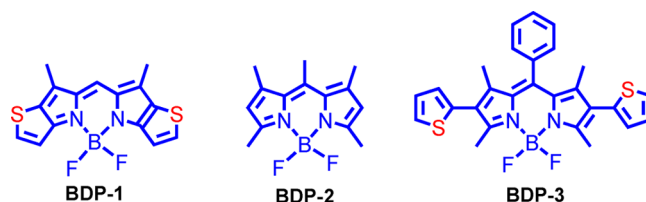
Triplet photosensitizers are versatile compounds that have been widely used in photodynamic therapy (PDT),¹ as photocatalysts in photocatalytic H₂ production and photoredox organic reactions,² and in photoinduced charge separation^{3a–c} and triplet–triplet annihilation upconversion.^{3d–g} Triplet photosensitizers play the pivotal role by first harvesting light, leading to the singlet excited state, and then promoting the formation of the triplet state via intersystem crossing (ISC). Finally, they may trigger intermolecular electron- or energy-transfer processes. In order to facilitate ISC, the most well-known approach is to take advantage of the heavy-atom effect, obtained with metallic coordination centers such as Ir(III), Pt(II), and Ru(II) or alternatively with iodine atoms.⁴ The heavy-atom effect is proportional to the atomic number, Z^4 . As a consequence, a larger heavy-atom effect is expected for Pt or Ir than for S or Br.⁴ It is indeed well-known that most of the Ir(III), Pt(II), and Ru(II) transition-metal complexes show efficient and ultrafast ISC.⁵ For example, Ru(bpy)₃Cl₂ (bpy = 2,2'-bipyridine) displays a quantum yield for triplet-state formation of 100%. Previously it was also shown that iodine substitution on the π core of the boron–dipyrromethene (BODIPY) chromophore is an effective approach to access efficient organic triplet photosensitizers.⁶

Significant heavy-atom effects obtained with nonmetallic atoms other than iodine remain scarce, though designing efficient triplet photosensitizers with lighter atoms, such as sulfur, would be of tremendous interest. While some oligothiophene compounds are known to form triplet excited states upon photoexcitation, this effect has not been thoroughly

studied for small molecules that contain thiophene moieties.^{7a,b} During the preparation of this article, a thiophene-fused BODIPY derivative was reported to show ISC capability, but the detailed mechanism was not studied.^{7c}

Recently a thiophene-fused BODIPY dye, BDP-1 (Scheme 1), was reported to show very weak fluorescence,^{8a} whereas

Scheme 1. Compounds Used in This Study



BODIPY compounds normally show strong fluorescence.^{8b–d} We consequently envisioned that efficient ISC could be attained with this compound. Herein we present the synthesis and spectroscopic characterization of this BODIPY derivative. The generation of triplet excited states was confirmed by nanosecond transient absorption spectroscopy and rationalized on the basis of ab initio calculations. We found that triplet formation with heavy-atom-free BDP-1 is more efficient (triplet-state formation quantum yield $\Phi_T = 63.7\%$) than

Received: March 31, 2015

Published: May 5, 2015

with the BODIPY derivative **BDP-3** presenting nonfused thiophene rings ($\Phi_T = 6.1\%$). Theoretical calculations showed that for **BDP-1** a higher-lying triplet state (i.e., T_2) that is energetically aligned to the spectroscopic S_1 state is responsible for the enhanced ISC processes. In short, we demonstrate that the incorporation of sulfur atoms into the π -conjugated skeleton of BODIPY is an efficient approach to attain high quantum yields for triplet-state formation.

The UV–vis absorption spectra of the compounds were studied (Figure 1). **BDP-1** shows a strong absorption at 571

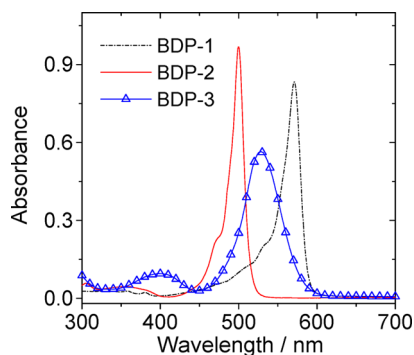


Figure 1. UV–vis absorption spectra of **BDP-1**, **BDP-2**, and **BDP-3** ($c = 1.0 \times 10^{-5}$ M in toluene, 20 °C).

nm. In comparison, **BDP-3** shows a blue-shifted absorption band peaking at 529 nm. **BDP-1** undergoes a very slight blue shift in polar solvents compared with nonpolar solvents (Figure S7 in the Supporting Information (SI)). This result indicates that the ground state presents a larger dipole moment than the first singlet excited states. Similar results were observed for both **BDP-2** and **BDP-3** (see Figure S7).

Fluorescence spectra were also recorded (Figure 2). **BDP-1** shows weak fluorescence ($\Phi_F = 4.0\%$). **BDP-3** shows red-

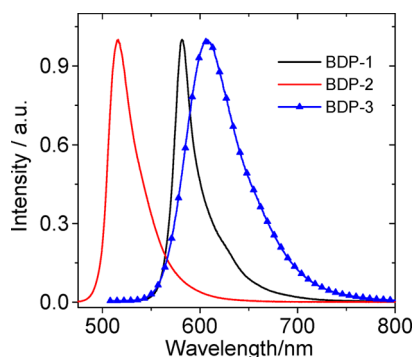


Figure 2. Normalized emission spectra of **BDP-1** (black, $\lambda_{ex} = 530$ nm, $A_{530} = 0.20$), **BDP-2** (red, $\lambda_{ex} = 470$ nm, $A_{470} = 0.26$), and **BDP-3** (blue, $\lambda_{ex} = 498$ nm, $A_{498} = 0.23$) in toluene at 20 °C.

shifted emission at 608 nm and a larger Stokes shift. **BDP-2** fluoresces at 516 nm. This experimental evidence is in agreement with extended π conjugation in **BDP-1** compared with **BDP-3**.

To investigate generation of the triplet state in **BDP-1**, nanosecond transient absorption spectra were recorded (Figure 3). Upon pulsed laser excitation, a bleaching band at 566 nm was observed. Excited-state absorption (ESA) at 491 nm was also observed. The lifetime of the transient was determined to be 170.5 μ s. The transient was significantly quenched in aerated

solution, and hence, it is related to the formation of a triplet excited state (Figure S18 in the SI). The triplet-state quantum yield (Φ_T) of **BDP-1**, as determined with the singlet-state depletion method, amounts to 63.7% (see Table 1). No significant triplet-state formation was observed in **BDP-2** (Φ_T is negligible). A similar nanosecond transient absorption spectrum was observed for **BDP-3** (see Figure S17 in the SI). However, a lower triplet-state quantum yield was observed for **BDP-3** ($\Phi_T = 6.1\%$) than for **BDP-1**. The photophysical properties of the compounds are summarized in Table 1.

In order to rationalize the different ISC rates in **BDP-1**, **BDP-2**, and **BDP-3**, the relative energies of the singlet and triplet states as well as the spin–orbit coupling (SOC) in the compounds were studied. The rate of ISC between the n th singlet (S_n) and m th triplet (T_m) excited states (k_{ISC}) obeys the empirical equation known as Fermi's Golden Rule (eq 1):

$$k_{ISC} = \frac{2\pi}{\hbar} \langle S_n | \hat{H}_{SO} | T_m \rangle^2 \times [\text{FCWD}] \quad (1)$$

where the bracket factor stands for the associated SOC and [FCWD] denotes the Franck–Condon weighted density of states. From a computational viewpoint, the calculation of ISC rates first requires the assignment of the main photo-deactivation channels followed by accurate calculations of (i) relative energy levels of the involved excited states, (ii) SOC matrix elements, (iii) vibrational frequencies, and (iv) Huang–Rhys factors. Computing all of the parameters in eq 1 becomes rapidly prohibitive for large molecules.⁹ Instead, semiquantitative and qualitative strategies are often used to rationalize the efficiency of ISC processes.¹⁰ On the basis of the computation of k_{ISC} values relying on accurate ab initio electronic structure data, it has been concluded that two main factors, i.e., substantial electronic and/or vibronic SOC and small T_m – S_n energy gaps, govern the efficiency of ISC processes.⁹ Herein we report theoretical estimates of SOCs and relative T_m – S_n energy gaps to rationalize the efficient ISC in **BDP-1** compared with that in both **BDP-2** and **BDP-3**. Modeling the properties of electronically excited states of BODIPY dyes is still a significant challenge for quantum-chemical methods because of the well-documented *cyanine challenge*, which is rooted in the need to capture large differential electron correlation effects in these compounds.¹¹ Recent time-dependent density functional theory (TD-DFT) studies of the excited states of BODIPY dyes concluded that among the available pool of exchange–correlation functionals, M06-2X outperforms the others.¹² However, TD-DFT still systematically overshoots the transition energies of BODIPY dyes by ca. 0.4 eV. Therefore, correction of the TD-DFT values with transition energies obtained at the scaled-opposite-spin configuration interaction singles with doubles corrections (SOS-CIS(D)) level has been advocated as a much more accurate approach.¹³

Table 2 lists the TD-M06-2X and SOS-CIS(D) vertical excitation energies for the lowest singlet and triplet excited states of **BDP-1**, **BDP-2**, and **BDP-3** at their optimized ground-state geometries (for computational details, see the SI). As expected, the SOS-CIS(D) excitation energies of the spectroscopic state (S_1) are in better agreement with the position of the measured UV–vis absorption bands (see Table 2). Regarding their intensities, **BDP-1** shows a higher oscillator strength than **BDP-3**, in accordance with the experimental evidence. TD-M06-2X systematically overestimates and underestimates the excitation energies of the singlet and triplet excited states by ca. +0.4 and –0.25 eV, respectively, compared

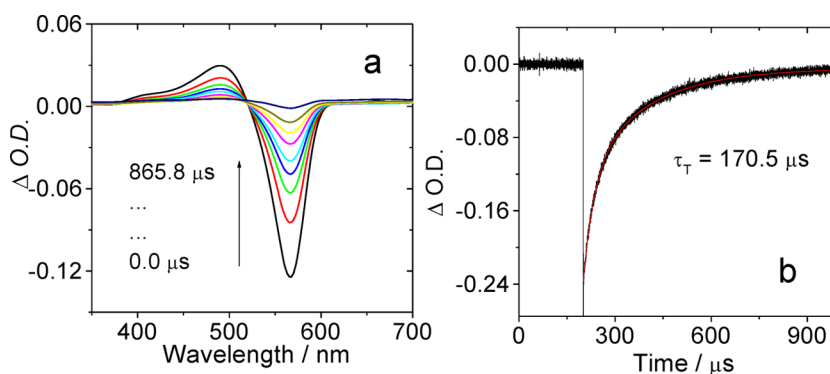


Figure 3. (a) Nanosecond transient absorption of BDP-1 after pulsed laser excitation ($\lambda_{\text{ex}} = 560$ nm) and (b) decay trace of BDP-1 at 569 nm in deaerated toluene ($c = 1.0 \times 10^{-5}$ M, 20 °C).

Table 1. Photophysical Parameters of the Compounds

	λ_{abs}^a	ϵ^b	$\lambda_{\text{em}} (\text{eV})^c$	$\Phi_{\text{F}} (\%)^d$	$\tau_{\text{F}} (\text{ns})^e$	$\tau_{\text{T}} (\mu\text{s})^f$	$\Phi_{\Delta} (\%)^g$	$\Phi_{\text{T}} (\%)^h$
BDP-1	571 nm (2.17 eV)	8.35	582 nm (2.13 eV)	4.0 ⁱ	1.35	170.5	58.1	63.7
BDP-2	500 nm (2.48 eV)	9.71	516 nm (2.41 eV)	99.0 ⁱ	5.30	–	–	–
BDP-3	529 nm (2.35 eV)	5.65	608 nm (2.04 eV)	11.2	4.59	389.9	4.93	6.1

^aIn toluene (1.0×10^{-5} M). ^bMolar extinction coefficient at the absorption maximum in units of $10^4 \text{ M}^{-1} \text{ cm}^{-1}$. ^cIn toluene. ^dFluorescence quantum yields. Diiodo-BODIPY ($\Phi_{\text{F}} = 0.027$ in CH_3CN) was used as a standard. ^eLuminescence lifetimes in toluene with $\lambda_{\text{ex}} = 405$ nm at RT. ^fTriplet-state lifetimes determined by nanosecond time-resolved transient absorption spectroscopy (BDP-1, $\lambda_{\text{ex}} = 560$ nm; BDP-3, $\lambda_{\text{ex}} = 532$ nm) at 1.0×10^{-5} M in deaerated toluene. ^gQuantum yields of singlet oxygen ($^1\text{O}_2$) obtained using diiodo-BODIPY as a standard ($\Phi_{\Delta} = 0.83$ in CH_2Cl_2) at 1.0×10^{-5} M in CH_2Cl_2 . ^hTriplet-state quantum yields upon direct photoexcitation at 462 nm using $\text{Ru}(\text{bpy})_3\text{Cl}_2$ ($\Phi_{\text{T}} = 1.0$ in H_2O) as a standard. ⁱLiterature value.^{6b,8a}

Table 2. Lowest Vertical Singlet and Triplet Electronic Transition Energies (in eV) and Oscillator Strengths (in Parentheses) of BDP-1, BDP-2, and BDP-3 at the TD-M06-2X and SOS-CIS(D) Levels of Theory, Along with Vertical Singlet–Triplet Splittings (in eV) and SOCs between the Involved T_m and S_1 States (in cm^{-1})

	state/assignment ^a	TD-M06-2X	SOS-CIS(D)	$\Delta E_{\text{SOS-CIS(D)}} (S_1-T_m)$	$\langle S_1 \hat{H}_{\text{SO}} T_m \rangle^b$
BDP-1	S_1 (H \rightarrow L, $c = 0.67$; H-1 \rightarrow L, $c = -0.20$)	2.72 (0.913)	2.32	–	–
	T_1 (H \rightarrow L, $c = 0.72$)	1.24	1.50	0.82	(0.0; 0.0; -3.2)
	T_2 (H-1 \rightarrow L, $c = 0.68$)	2.35	2.56	-0.24	(-1.2; -1.3; 0.0)
BDP-2	S_1 (H \rightarrow L, $c = 0.70$)	2.99 (0.539)	2.51	–	–
	T_1 (H \rightarrow L, $c = 0.71$)	1.60	1.83	0.68	(-0.3; 0.0; 0.0)
BDP-3	S_1 (H \rightarrow L, $c = 0.70$)	2.76 (0.772)	2.29	–	–
	T_1 (H \rightarrow L, $c = 0.69$)	1.50	1.73	0.56	(-0.4; -0.2; 0.2)

^aOnly the excited states that are below the experimental λ_{ex} of the photoexcitation are considered ($\lambda_{\text{ex}} = 462$ nm/2.68 eV). ^bValues are shown as (x component; y component; z component) and were obtained at the QR-TD-DFT/6-31G* level of theory at the T_1 optimized geometry.

with SOS-CIS(D). In view of this evidence, we discuss only the SOS-CIS(D) values in the following. To evaluate the main $S_n \rightarrow T_m$ ISC channels, only the excited states that are below the experimental λ_{ex} of the photoexcitation are considered ($\lambda_{\text{ex}} = 462$ nm/2.68 eV; see Table 1). Upon photoexcitation, there are two possible $S_n \rightarrow T_m$ ISC channels for the spectroscopic state (S_1) of BDP-1, i.e., $S_1 \rightarrow T_2$ and $S_1 \rightarrow T_1$. Because of the smaller energetic gap between T_2 and S_1 (i.e., 0.24 eV; see Table 2), we propose $S_1 \rightarrow T_2$ to be the most important triplet deactivation channel for BDP-1. In contrast, for BDP-2 and BDP-3 only the $S_1 \rightarrow T_1$ ISC channel is energetically accessible. Table 2 also collects the SOCs between the involved T_m and S_1 excited states obtained by quadratic response (QR)-TD-DFT/6-31G* calculations (see the SI). As expected for organic compounds, the SOCs amount only to a few cm^{-1} . As shown in Table S3 in the SI, the effect of increasing the size of the basis set on the SOCs calculations is almost negligible, so the results are almost converged at the (QR)-TD-DFT/6-31G* level of theory. It should be recalled that SOC values between

0.2 and 5.0 cm^{-1} are considered large enough to induce ISC on a nanosecond time scale.¹⁴

The SOCs in BDP-1 are 1 order of magnitude larger than those in the two other dyes since the sulfur atom contributes to the involved lowest excited states of BDP-1 (see the assignment of the excited states in Table 2 and the involved orbitals in Figure 4). In BDP-3 the sulfur atoms located in the peripheral ligands do not contribute to the BODIPY-like excited states (see Table 2 and Figure 4). Therefore, since BDP-1 possesses the largest SOCs and the smallest singlet–triplet energy gap among all of the BODIPY dyes, it will easily undergo photodeactivation through ISC. Indeed, as discussed above, BDP-1 yields the largest quantum yields of singlet oxygen (Φ_{Δ}) and triplet generation (Φ_{T}) (see Table 1). Comparison of BDP-3 with BDP-2 is more qualitative, though the slightly increased SOCs and the lower singlet–triplet energy gaps in BDP-3 compared with BDP-2 point to slightly increased ISC channels for the latter, in accordance with the experimental observations.

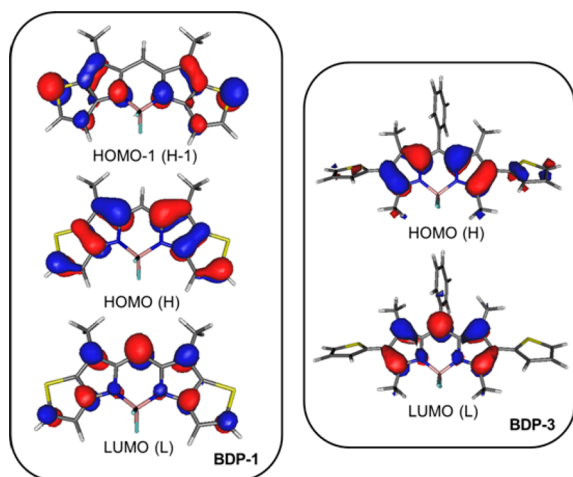


Figure 4. Kohn–Sham orbitals (M06-2X/6-311+G(2d,p)) involved in the lowest excited states of BDP-1 and BDP-3.

In summary, we have found that a heavy-atom-free thiophene-fused BODIPY, BDP-1, shows efficient ISC with a triplet-state quantum yield (Φ_T) of 63.7%. In comparison, two reference BODIPY derivatives that contain either no sulfur atom (BDP-2) or thiophene groups not participating directly in the π -conjugation pathway of the BODIPY core (BDP-3) do not show any significant ISC (Φ_T is negligible for BDP-2 and is only 6.1% for BDP-3). Theoretical calculations demonstrated that the increased ISC mechanisms for BDP-1 compared with BDP-2 and BDP-3 are due to (i) the participation of the sulfur atom in the lowest-lying excited states, which leads to moderate SOC, and (ii) the small singlet–triplet energy gap in BDP-1. These insights are useful in designing heavy-atom-free triplet photosensitizers and understanding the fundamental photochemistry of the ISC mechanisms of organic chromophores.

EXPERIMENTAL SECTION

General Remarks. All of the chemicals were analytically pure and used as received. Solvents were dried and distilled prior to use. Fluorescence lifetimes were measured with an OB920 luminescence lifetime spectrometer (Edinburgh, U.K.). Compound BDP-1 was prepared following the reported method.^{8a} BDP-2 and BDP-3 were reported previously.¹⁵

Compound 2. Into a 100 mL flask (dry, under Ar) was placed CH_2Cl_2 (30 mL), and the flask was cooled using an ice bath before AlCl_3 (4.9 g, 36.8 mmol) was added. A dropping funnel was charged with acetyl chloride (2.68 mL, 39.2 mmol) in CH_2Cl_2 (30 mL), and this solution was added to the AlCl_3 suspension over a period of 10 min. After about 30 min of stirring at 0 °C, most of the AlCl_3 had dissolved. A second dropping funnel was charged with 3-bromothiophene (0.574 mL, 1.00 g, 6.13 mmol) in CH_2Cl_2 (30 mL), and this mixture was added to the reaction mixture over a 10 min period. The reaction was left to proceed at 0 °C for 30 min, and then the reaction mixture was warmed slowly to room temperature (RT) for another hour. Then the reaction mixture was cooled to 0 °C once again, and water was added carefully. The reaction mixture was diluted with CH_2Cl_2 , and water was added. The water layer was extracted twice with CH_2Cl_2 , washed with saturated NaHCO_3 and brine, and finally dried over anhydrous MgSO_4 . Evaporation of the solvent and purification by column chromatography (hexane: CH_2Cl_2 = 1:1) gave compound 2 as a yellow liquid (2.4 g, 98%). $^1\text{H NMR}$ (CDCl_3 , 400 MHz): δ 7.55 (d, J = 4.9 Hz, 1H), 7.10 (d, J = 5.2 Hz, 1H), 2.68 (s, 3H).

Compound 3. To a mixture containing 2 (204 mg, 1 mmol), CuI (19 mg, 0.1 mmol), and Cs_2CO_3 (651 mg, 2 mmol) in DMSO (1 mL) was added ethyl isocyanoacetate (124 mg, 1.1 mmol) dropwise at RT.

After 4 h of stirring at 50 °C, the reaction mixture was extracted with CH_2Cl_2 . The organic layer was washed with brine twice, and then the organic layer was dried over MgSO_4 and filtered. The filtrate was condensed with evaporation, and silica gel column chromatography with a mixed eluent (hexane:ethyl acetate = 9:1) gave compound 3 as a white solid (110 mg, 53%). $^1\text{H NMR}$ (400 MHz, CDCl_3): δ 8.94 (s, 1H), 7.31 (d, J = 5.3 Hz, 1H), 6.91 (d, J = 5.3 Hz, 1H), 4.40 (q, J = 7.2 Hz, 2H), 2.52 (s, 3H), 1.41 (t, J = 7.2 Hz, 3H).

Compound 4. A mixture containing 3 (340 mg, 1.63 mmol) and aqueous NaOH solution (1.032 g in 7.2 mL of H_2O) in 13.5 mL of ethanol was refluxed for 1 h and then cooled to RT, and HCl (10%) was added dropwise to acidify it. The products were extracted with CH_2Cl_2 , and the organic layer was washed with brine, dried over MgSO_4 , and filtered. Evaporation of the filtrate yielded compound 4 as a dark-purple solid (268 mg, 90%). $^1\text{H NMR}$ (400 MHz, $\text{DMSO}-d_6$): δ 12.43 (s, 1H), 11.51 (s, 1H), 7.47 (d, J = 5.2 Hz, 1H), 6.94 (d, J = 5.3 Hz, 1H), 2.41 (s, 3H).

Compound 5. A solution of 4 (150 mg, 0.83 mmol) dissolved in trifluoroacetic acid (2.7 mL) was stirred at 50 °C for 20 min, and then triethyl orthoformate (512 mg, 3.46 mmol) was added. After 30 min of stirring at 50 °C, excess amounts of diethyl ether and saturated aqueous NaHCO_3 were poured into the reaction solution. The organic layer was washed with brine and water, dried over MgSO_4 , filtered, and condensed by evaporation to afford 5 as a brown solid (110 mg, 80.4%). $^1\text{H NMR}$ (500 MHz, CDCl_3): δ 9.75 (s, 1H), 9.08 (s, 1H), 7.45 (d, J = 5.2 Hz, 1H), 6.95 (d, J = 5.2 Hz, 1H), 2.54 (s, 3H).

Compound BDP-1. To a solution of 5 (200 mg, 1.2 mmol) in CH_2Cl_2 was added POCl_3 (227 mg, 1.5 mmol) dropwise at 0 °C. After 3 days of stirring at room temperature in the dark, triethylamine (0.84 mL, 6 mmol) was added dropwise at 0 °C. After 15 min of stirring at 0 °C, $\text{BF}_3\cdot\text{Et}_2\text{O}$ (1.1 mL, 8.9 mmol) was added dropwise, and then the mixture was stirred at room temperature for 2 days. The reaction was quenched by the addition of 10 mL of water, and the products were extracted with CH_2Cl_2 . The organic layer was washed with water twice and brine, dried over MgSO_4 , filtered, and condensed by evaporation. The residue was passed through a silica gel column with a mixed eluent (hexane: CH_2Cl_2 = 5:1) to afford BDP-1 as a dark-purple solid (10 mg, 5%). $^1\text{H NMR}$ (CDCl_3 , 500 MHz): δ 7.64 (d, J = 5.3 Hz, 2H), 7.38 (s, 1H), 7.12 (d, J = 5.3 Hz, 2H), 2.42 (s, 6H). TOF HRMS EI^+ : calcd ($[\text{C}_{15}\text{H}_{11}\text{BF}_2\text{N}_2\text{S}_2]^+$) m/z = 332.0425, found m/z = 332.0417.

Theoretical Computations. The geometries of the singlet ground states (S_0) of BDP-1, BDP-2, and BDP-3 were optimized at the M06-2X/6-31G(d) level of theory. Gas-phase TD-M06-2X and SOS-CIS(D) vertical singlet and triplet excitation energies were obtained at this geometry using the 6-311+G(2d,p) and 6-31+G(d) basis sets, respectively. The geometries of the lowest singlet (S_1) and triplet (T_1) excited states were also optimized at the TD-M06-2X/6-31G(d) level of theory. SOC were computed using the quadratic-response TD-DFT approach¹⁶ (i.e., QR-TD-DFT) as implemented in the Dalton program¹⁷ at their T_1 optimized geometries. The SOC operator made use of a semiempirical effective single-electron approximation.¹⁸ For the latter calculations, the B3LYP functional in combination with the 6-31G(d) basis set was used. SOS-CIS(D) and TD-DFT calculations were carried out with the Q-Chem¹⁹ and Gaussian 09²⁰ program packages, respectively.

Triplet-State Quantum Yield (Φ_T). The triplet-state quantum yields were determined by the singlet-state depletion method.²¹ The Φ_T values were obtained by comparing ΔA_S for the optically matched sample solution at 452 nm in a 1 cm cuvette to that of the reference $\text{Ru}(\text{bpy})_3\text{Cl}_2$ solution using eq 2:

$$\Phi_T = \Phi_T^{\text{Ru}} \frac{\epsilon_S^{\text{Ru}} \Delta A_S}{\epsilon_S \Delta A_S^{\text{Ru}}} \quad (2)$$

where the superscript “Ru” represents the reference, ΔA_S is the absorbance change of the triplet transient difference absorption spectrum at the minimum of the bleaching band, and ϵ_S is the ground-state molar absorption coefficient at the UV–vis absorption band maximum.

■ ASSOCIATED CONTENT

Supporting Information

Molecular structure characterization, additional spectra, atom coordinates, absolute energies of the optimized geometries, and more computational details. The Supporting Information is available free of charge on the ACS Publications website at DOI: 10.1021/acs.joc.5b00691.

■ AUTHOR INFORMATION

Corresponding Authors

*E-mail: smji@xtu.edu.cn (S.J.)

*E-mail: zhaojzh@dlut.edu.cn (J.Z.)

*E-mail: Denis.Jacquemin@univ-nantes.fr (D.J.)

Notes

The authors declare no competing financial interest.

■ ACKNOWLEDGMENTS

S.J. thanks the NNSFC (51202207), and J.Z. thanks the NNSFC (21273028, 21473020, and 21421005), the Ministry of Education (SRFDP-20120041130005), the Fundamental Research Funds for the Central Universities (DUT14ZD226), the Program for Changjiang Scholars and Innovative Research Team in University (IRT_132206), and Dalian University of Technology (DUT2013TB07) for financial support. D.E. acknowledges the European Research Council (ERC, Marches-278845) and the Région des Pays de la Loire for his postdoctoral grant. D.J. acknowledges the European Research Council (ERC) and the Région des Pays de la Loire for financial support in the framework of a starting grant (Marches-278845) and a Recrutement sur Poste Stratégique, respectively. This research used resources of (1) the GENCI-CINES/IDRIS, (2) Centre de Calcul Intensif des Pays de la Loire (CCIPL), and (3) a local Troy cluster.

■ REFERENCES

- (1) (a) Kamkaew, A.; Lim, S. H.; Lee, H. B.; Kiew, L. V.; Chung, L. Y.; Burgess, K. *Chem. Soc. Rev.* **2013**, *42*, 77–88. (b) Awuah, S. G.; You, Y. *RSC Adv.* **2012**, *2*, 11169–11183. (c) Zhao, J.; Wu, W.; Sun, J.; Guo, S. *Chem. Soc. Rev.* **2013**, *42*, 5323–5351.
- (2) (a) Shi, L.; Xia, W. *Chem. Soc. Rev.* **2012**, *41*, 7687–7697. (b) Hari, D. P.; König, B. *Angew. Chem., Int. Ed.* **2013**, *52*, 4734–4743. (c) McNamara, W. R.; Han, Z.; Alperin, P. J.; Brennessel, W. W.; Holland, P. L.; Eisenberg, R. *J. Am. Chem. Soc.* **2011**, *133*, 15368–15371.
- (3) (a) Bandi, V.; Das, S. K.; Awuah, S. G.; You, Y.; D'Souza, F. *J. Am. Chem. Soc.* **2014**, *136*, 7571–7574. (b) D'Souza, F.; Amin, A. N.; El-Khouly, M. E.; Subbaiyan, N. K.; Zandler, M. E.; Fukuzumi, S. *J. Am. Chem. Soc.* **2012**, *134*, 654–664. (c) Bill, N. L.; Ishida, M.; Bähring, S.; Lim, J. M.; Lee, S.; Davis, C. M.; Lynch, V. M.; Nielsen, K. A.; Jeppesen, J. O.; Ohkubo, K.; Fukuzumi, S.; Kim, D.; Sessler, J. L. *J. Am. Chem. Soc.* **2013**, *135*, 10852–10862. (d) Singh-Rachford, T. N.; Castellano, F. N. *Coord. Chem. Rev.* **2010**, *254*, 2560–2573. (e) Zhao, J.; Ji, S.; Guo, H. *RSC Adv.* **2011**, *1*, 937–950. (f) Liu, Q.; Yang, T.; Feng, W.; Li, F. *J. Am. Chem. Soc.* **2012**, *134*, 5390–5397. (g) Singh-Rachford, T. N.; Nayak, A.; Muro-Small, M. L.; Goeb, S.; Therien, M. J.; Castellano, F. N. *J. Am. Chem. Soc.* **2010**, *132*, 14203–14211.
- (4) Turro, N. J.; Ramamurthy, V.; Scaiano, J. C. *Principles of Molecular Photochemistry: An Introduction*; University Science Books: Sausalito, CA, 2009.
- (5) (a) Wong, K. M.-C.; Yam, V. W.-W. *Coord. Chem. Rev.* **2007**, *251*, 2477–2488. (b) Williams, J. A. G. *Top. Curr. Chem.* **2007**, *281*, 205–268. (c) Chou, P.-T.; Chi, Y.; Chung, M.-W.; Lin, C.-C. *Coord. Chem. Rev.* **2011**, *255*, 2653–2665. (d) Ho, C.-L.; Wong, W.-Y.; Gao, Z.-Q.; Chen, C.-H.; Cheah, K.-W.; Yao, B.; Xie, Z.; Wang, Q.; Ma, D.; Wang, L.; Yu, X.-M.; Kwok, H.-S.; Lin, Z. *Adv. Funct. Mater.* **2008**, *18*, 319–

331. (e) Lamansky, S.; Djurovich, P.; Murphy, D.; Abdel-Razzaq, F.; Lee, H.-E.; Adachi, C.; Burrows, P. E.; Forrest, S. R.; Thompson, M. E. *J. Am. Chem. Soc.* **2001**, *123*, 4304–4312. (f) Schanze, K. S.; Silverman, E. E.; Zhao, X. *J. Phys. Chem. B* **2005**, *109*, 18451–18459. (g) Escudero, D.; Jacquemin, D. *Dalton Trans.* **2015**, *44*, 8346–8355.
- (6) (a) Yogo, T.; Urano, Y.; Ishitsuka, Y.; Maniwa, F.; Nagano, T. *J. Am. Chem. Soc.* **2005**, *127*, 12162–12163. (b) Wu, W.; Guo, H.; Wu, W.; Ji, S.; Zhao, J. *J. Org. Chem.* **2011**, *76*, 7056–7064.
- (7) (a) Wasserberg, D.; Marsal, P.; Meskers, S. C. J.; Janssen, R. A. J.; Beljonne, D. *J. Phys. Chem. B* **2005**, *109*, 4410–4415. (b) Janssen, R. A. J.; Smilowitz, L.; Sariciftci, N. S.; Moses, D. *J. Chem. Phys.* **1994**, *101*, 1787–1798. (c) Watley, R. L.; Awuah, S. G.; Bio, M.; Cantu, R.; Gobeze, H. B.; Nesterov, V. N.; Das, S. K.; D'Souza, F.; You, Y. *Chem.—Asian J.* **2015**, DOI: 10.1002/asia.201500140.
- (8) (a) Tanaka, K.; Yamane, H.; Yoshii, R.; Chujo, Y. *Bioorg. Med. Chem.* **2013**, *21*, 2715–2719. (b) Guliyev, R.; Coskun, A.; Akkaya, E. U. *J. Am. Chem. Soc.* **2009**, *131*, 9007–9013. (c) Loudet, A.; Burgess, K. *Chem. Rev.* **2007**, *107*, 4891–4932. (d) Ulrich, G.; Ziessel, R.; Harriman, A. *Angew. Chem., Int. Ed.* **2008**, *47*, 1184–1201.
- (9) Marian, C. M. *Wiley Interdiscip. Rev.: Comput. Mol. Sci.* **2012**, *2*, 187–203.
- (10) Li, E. Y.-T.; Jiang, T.-Y.; Chi, Y.; Chou, P.-T. *Phys. Chem. Chem. Phys.* **2014**, *16*, 26184–26192.
- (11) Le Guennic, B.; Jacquemin, D. *Acc. Chem. Res.* **2015**, *48*, 530–537.
- (12) (a) Chibani, S.; Le Guennic, B.; Charaf-Eddin, A.; Maury, O.; Andraud, C.; Jacquemin, D. *J. Chem. Theory Comput.* **2012**, *8*, 3303–3313. (b) Chibani, S.; Le Guennic, B.; Charaf-Eddin, A.; Laurent, A. D.; Jacquemin, D. *Chem. Sci.* **2013**, *4*, 1950–1963.
- (13) (a) Chibani, S.; Laurent, A. D.; Le Guennic, B.; Jacquemin, D. *J. Chem. Theory Comput.* **2014**, *10*, 4574–4582. (b) Alberto, M. E.; De Simone, B. C.; Mazzone, G.; Quartarolo, A. D.; Russo, N. *J. Chem. Theory Comput.* **2014**, *10*, 4006–4013.
- (14) Klessinger, M. *Theor. Comput. Chem.* **1998**, *5*, 581–610.
- (15) Chen, Y.; Zhao, J.; Xie, L.; Guo, H.; Li, Q. *RSC Adv.* **2012**, *2*, 3942–3953.
- (16) (a) Rinkevicius, Z.; Tunell, I.; Salek, P.; Vahtras, O.; Ågren, H. *J. Chem. Phys.* **2003**, *119*, 34–46. (b) Ågren, H.; Vahtras, O.; Minaev, B. *Adv. Quantum Chem.* **1996**, *27*, 71–162.
- (17) Helgaker, T.; Jørgensen, P.; Olsen, J.; Ruud, K.; Andersen, T.; Bak, K. L.; Bakken, V.; Christiansen, O.; Dahle, P.; Dalskov, E. K.; Enevoldsen, T.; Heiberg, H.; Hetttema, H.; Jonsson, D.; Kirpekar, S.; Kobayashi, R.; Koch, H.; Mikkelsen, K. V.; Norman, P.; Packer, M. J.; Saue, T.; Taylor, P. R.; Vahtras, O.; Jensen, H. J. A.; Ågren, H. *Dalton: An Ab Initio Electronic Structure Program*, version 1.0, 1997.
- (18) Koseki, S.; Schmidt, M. W.; Gordon, M. S. *J. Phys. Chem.* **1992**, *96*, 10768–10772.
- (19) Shao, Y.; Molnar, L. F.; Jung, Y.; Kussmann, J.; Ochsenfeld, C.; Brown, S. T.; Gilbert, A. T. B.; Slipchenko, L. V.; Levchenko, S. V.; O'Neill, D. P.; DiStasio, R. A., Jr.; Lochan, R. C.; Wang, T.; Beran, G. J. O.; Besley, N. A.; Herbert, J. M.; Lin, C. Y.; Van Voorhis, T.; Chien, S. H.; Sodt, A.; Steele, R. P.; Rassolov, V. A.; Maslen, P. E.; Korambath, P. P.; Adamson, R. D.; Austin, B.; Baker, J.; Byrd, E. F. C.; Dachsel, H.; Doerksen, R. J.; Dreuw, A.; Dunietz, B. D.; Dutoi, A. D.; Furlani, T. R.; Gwaltney, S. R.; Heyden, A.; Hirata, S.; Hsu, C.-P.; Kedziora, G.; Khalliulin, R. Z.; Klunzinger, P.; Lee, A. M.; Lee, M. S.; Liang, W.; Lotan, I.; Nair, N.; Peters, B.; Proynov, E. I.; Pieniazek, P. A.; Rhee, Y. M.; Ritchie, J.; Rosta, E.; Sherrill, C. D.; Simmonett, A. C.; Subotnik, J. E.; Woodcock, H. L., III; Zhang, W.; Bell, A. T.; Chakraborty, A. K.; Chipman, D. M.; Keil, F. J.; Warshel, A.; Hehre, W. J.; Schaefer, H. F., III; Kong, J.; Krylov, A. I.; Gill, P. M. W.; Head-Gordon, M. *Phys. Chem. Chem. Phys.* **2006**, *8*, 3172–3191.
- (20) Frisch, M. J.; Trucks, G. W.; Schlegel, H. B.; Scuseria, G. E.; Robb, M. A.; Cheeseman, J. R.; Scalmani, G.; Barone, V.; Mennucci, B.; Petersson, G. A.; Nakatsuji, H.; Caricato, M.; Li, X.; Hratchian, H. P.; Izmaylov, A. F.; Bloino, J.; Zheng, G.; Sonnenberg, J. L.; Hada, M.; Ehara, M.; Toyota, K.; Fukuda, R.; Hasegawa, J.; Ishida, M.; Nakajima, T.; Honda, Y.; Kitao, O.; Nakai, H.; Vreven, T.; Montgomery, J. A., Jr.; Peralta, J. E.; Ogliaro, F.; Bearpark, M.; Heyd, J. J.; Brothers, E.; Kudin,

K. N.; Staroverov, V. N.; Kobayashi, R.; Normand, J.; Raghavachari, K.; Rendell, A.; Burant, J. C.; Iyengar, S. S.; Tomasi, J.; Cossi, M.; Rega, N.; Millam, J. M.; Klene, M.; Knox, J. E.; Cross, J. B.; Bakken, V.; Adamo, C.; Jaramillo, J.; Gomperts, R.; Stratmann, R. E.; Yazyev, O.; Austin, A. J.; Cammi, R.; Pomelli, C.; Ochterski, J. W.; Martin, R. L.; Morokuma, K.; Zakrzewski, V. G.; Voth, G. A.; Salvador, P.; Dannenberg, J. J.; Dapprich, S.; Daniels, A. D.; Farkas, Ö.; Foresman, J. B.; Ortiz, J. V.; Cioslowski, J.; Fox, D. J. *Gaussian 09*, revision A.1; Gaussian, Inc.: Wallingford, CT, 2009.

(21) Li, Y.; Dandu, N.; Liu, R.; Li, Z.; Kilina, S.; Sun, W. *J. Phys. Chem. C* **2014**, *118*, 6372–6384.